J|A|C|S ARTICLES

Published on Web 03/16/2010

Anatomy of a Red Copper Center: Spectroscopic Identification and Reactivity of the Copper Centers of *Bacillus subtilis* Sco and Its Cys-to-Ala Variants

Gnana S. Siluvai,[†] Mary Mayfield,[†] Mark J. Nilges,[‡] Serena DeBeer George,[§] and Ninian J. Blackburn*,[†]

Department of Science & Engineering, Oregon Health & Science University, Beaverton, Oregon 97006, Illinois EPR Research Center, Urbana, Illinois 61801, and Department of Chemistry and Chemical Biology, Cornell University, Ithaca, New York 14853

Received December 21, 2009; E-mail: ninian@comcast.net

Abstract: Sco is a mononuclear red copper protein involved in the assembly of cytochrome *c* oxidase. It is spectroscopically similar to red copper nitrosocyanin, but unlike the latter, which has one copper cysteine thiolate, the former has two. In addition to the two cysteine ligands (C45 and C49), the wild-type (WT) protein from *Bacillus subtilis* (hereafter named BSco) has a histidine (H135) and an unknown endogenous protein oxygen ligand in a distorted tetragonal array. We have compared the properties of the WT protein to variants in which each of the two coordinating Cys residues has been individually mutated to Ala, using UV/visible, Cu and S K-edge X-ray absorption, electron paramagnetic resonance, and resonance Raman spectroscopies. Unlike the Cu(II) form of native Sco, the Cu(II) complexes of the Cys variants are unstable. The copper center of C49A undergoes autoreduction to the Cu(I) form, which is shown by extended X-ray absorption fine structure to be composed of a novel two-coordinate center with one Cys and one His ligand. C45A rearranges to a new stable Cu(II) species coordinated by C49, H135 and a second His ligand recruited from a previously uncoordinated protein side chain. The different chemistry exhibited by the Cys variants can be rationalized by whether a stable Cu(I) species can be formed by autoredox chemistry. For C49A, the remaining Cys and His residues are *trans*, which facilitates the formation of the highly stable two-coordinate Cu(I) species, while for C45A such a configuration cannot be attained. Resonance Raman spectroscopy of the WT protein indicates a net weak Cu−S bond strength at ∼2.24 Å corresponding to the two thiolate−copper bonds, whereas the single variant C45A shows a moderately strong Cu−S bond at ∼2.16 Å. S K-edge data give a total covalency of 28% for both Cu−S bonds in the WT protein. These data suggest an average covalency per Cu−S bond lower than that observed for nitrosocyanin and close to that expected for type-2 Cu(II)−thiolate systems. The data are discussed relative to the unique Cu−S characteristics of cupredoxins, from which it is concluded that Sco does not contain highly covalent Cu−S bonds of the type expected for long-range electron-transfer reactivity.

Introduction

Mononuclear cupric thiolate centers in proteins are broadly categorized as blue, green, or red.[1−8] They all have a unique spectral property, i.e., intense, thiolate−Cu(II) electronic absorption features that reflect the covalency of the thiolate−copper bond which in turn can make major contributions to reactivity. Consequently, they possess novel colors and intriguing redox activities, and in general they carry out long-range electron-transfer reactions in which the electrons are transferred along a preferred pathway that includes the highly covalent Cu−S bond.[7,9−13] The red copper protein nitrosocyanin is a recent addition to this group,[5,14,15] but in contrast to the previously studied cases, its thiolate−copper bond is found to have a low

[†] Oregon Health & Science University.
[‡] Illinois EPR Research Center.
[§] Cornell University.

(1) Gray, H. B.; Malmstrom, B. G.; Williams, R. J. *J. Biol. Inorg. Chem.* **2000**, *5*, 551–559.
(2) Holm, R. H.; Kennepohl, P.; Solomon, E. I. *Chem. Rev.* **1996**, *96*, 2239–2314.
(3) Andrew, C. R.; Yeom, H.; Valentine, J. S.; Karlsson, B. G.; van Pouderoyen, G.; Canters, G. W.; Loehr, T. M.; Sanders-Loehr, J.; Bonander, N. *J. Am. Chem. Soc.* **1994**, *116*, 11489–11498.
(4) Andrew, C. R.; Sanders-Loehr, J. *Acc. Chem. Res.* **1996**, *29*, 365–372.
(5) Basumallick, L.; Sarangi, R.; DeBeer George, S.; Elmore, B.; Hooper, A. B.; Hedman, B.; Hodgson, K. O.; Solomon, E. I. *J. Am. Chem. Soc.* **2005**, *127*, 3531–3544.
(6) LaCroix, L. B.; Shadle, S. E.; Wang, Y.; Averill, B. A.; Hedman, B.; Hodgson, K. O.; Solomon, E. I. *J. Am. Chem. Soc.* **1996**, *118*, 7755–7768.
(7) Solomon, E. I. *Inorg. Chem.* **2006**, *45*, 8012–8025.
(8) Savelieff, M. G.; Wilson, T. D.; Elias, Y.; Nilges, M. J.; Garner, D. K.; Lu, Y. *Proc. Natl. Acad. Sci. U.S.A.* **2008**, *105*, 7919–7924.
(9) Shadle, S. E.; Penner-Hahn, J. E.; Schugar, H. J.; Hedman, B.; Hodgson, K. O.; Solomon, E. I. *J. Am. Chem. Soc.* **1993**, *115*, 767–776.
(10) Randall, D. W.; Gamelin, D. R.; LaCroix, L. B.; Solomon, E. I. *J. Biol. Inorg. Chem.* **2000**, *5*, 16–29.
(11) Glaser, T.; Hedman, B.; Hodgson, K. O.; Solomon, E. I. *Acc. Chem. Res.* **2000**, *33*, 859–868.
(12) Solomon, E. I.; Szilagyi, R. K.; DeBeer George, S.; Basumallick, L. *Chem. Rev.* **2004**, *104*, 419–458.
(13) Solomon, E. I.; Hedman, B.; Hodgson, K. O.; Dey, A.; Szilagyi, R. K. *Coord. Chem. Rev.* **2005**, *249*, 97–129.

covalency of 20%, and hence it is suggested to perform a catalytic function rather than interprotein electron transfer.[5]

Recently the Sco family of copper regulators has been identified as containing a type 2 red copper center, and its members have been found to be spectroscopically similar to nitrosocyanin[16−21] but having a ligand set comprised of two cysteines, one histidine, and an as yet unidentified fourth ligand. Its function is still incompletely understood, though there is a clear involvement with the assembly of the multisubunit cytochrome *c* oxidase, in particular the subunit 2 which contains the Cu_A center. Mutagenesis of bacterial,[22] yeast,[23] or human[20] homologues has demonstrated that each of the three ligands to copper is essential for function. While it is possible that Sco mediates the transfer of copper into the Cu_A binuclear site, other functions for Sco proteins have been considered. For example, the structural homology to the thioredoxin family of thiol−disufide isomerases[17,24−26] has led to the hypothesis that Sco function is linked to thiol−disulfide redox[17,25] or redox signaling,[26] and since the Cu_A center is known to form a disulfide between the two bridging thiolates in the apoprotein, thioredoxin activity could conceivably be required to reduce the site to its copper-binding bis-cysteinate form. A recent study of the H135A variant of BSco has emphasized the importance of the Cu(II) form of the protein in function, leading to the suggestion that both Cu(II) and Cu(I) states (see Scheme 1) are required to metalate the mixed-valent Cu_A center and/or that Sco may serve a redox buffering function to protect the nascent metalated subunit 1 of cytochrome oxidase from damage due to accumulation of high-valent intermediates.[27]

These questions provide compelling reasons to study the Sco copper center in detail. First, understanding the active site structure and reactivity of Sco proteins will build a chemical framework in which to consider these functional alternatives. Second, Sco is unique among native mononuclear Cu(II)-containing proteins in having two copper−thiolate bonds, and while it is similar to nitrosocyanin, its chemistry and spectroscopy are largely unexplored. In addition, mutagenesis of one of its two cysteine residues to alanine or histidine generates a ligand set close to that found in type 1 copper proteins, which have been the subject of intense study due to their unusual electronic structures which in turn fine-tune their reactivity.[7] The unusual chemistry of the blue copper proteins has been largely ascribed to the uniqueness of the cupredoxin fold, which holds the copper binding site in a rigid protein matrix, allowing only minor perturbations to the coordinate structure. Sco provides a rare opportunity to examine protein-based copper−thiolate chemistry and spectroscopy in an unrelated protein scaffold.

Scheme 1. Cu(I) and Cu(II) Complexes of *Bacillus subtilis* Sco[a]

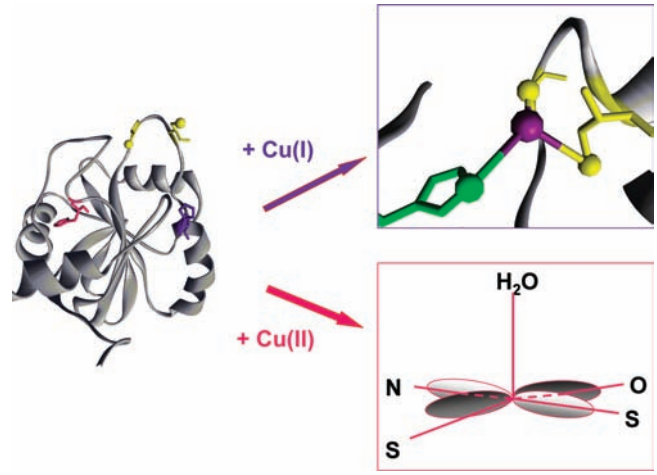

[a] Structure taken from PDB file 1ON4.

In previous work from our laboratory, the selectivity and the spectroscopic signatures of the bacterial Sco copper center from *B. subtilis* (BSco) were investigated.[19] In the present paper, we report on variants of BSco in which the copper−thiolate ligands C45 and C49 have been individually mutated to alanine or histidine, and studied by UV/visible, electron paramagnetic resonance (EPR), Cu and S K-edge X-ray absorption (XAS), and resonance Raman spectroscopies. Our results reveal that the Sco family possesses different chemistry and spectroscopy and lower Cu−S covalency than the well-studied cupredoxin family of electron-transfer proteins, leading to the conclusion that Sco is likely to play a catalytic and/or redox role rather than long-range electron transfer.

Materials and Methods

Mutagenesis of BSco, Protein Expression and Purification. The single variants of BSco, namely C45A and C49A, the double selenomethionine M52/M56-SeM (hereafter named WT-SeM), and the triple variants M52/M56-SeM/C45A (hereafter named C45A-SeM) were obtained via site-directed mutagenesis of constructs prepared in self-cleaving intein vectors (New England Biolabs pTXB3) as described previously.[19] All mutations were confirmed by DNA sequence analysis. Cell cultures of the single variants (expressing S(Met)-containing proteins) were grown in 1 L LB-glucose medium containing 100 μg/mL of ampicillin at 37 °C to a final OD_{600} between 0.6 and 0.8. Cell cultures of the double and triple SeM-containing variants were grown from the corresponding Met-minus strain B834(DE3) according to the earlier reported protocol.[28] The cells were initially grown as a small culture (10 mL) in LB media with ampicillin overnight at 37 °C. A 100 μL aliquot of this culture was used to inoculate 10 mL of enhanced minimal M9 medium supplemented with 2 mM $MgSO_4$, 0.1 mM

(14) Arciero, D. M.; Pierce, B. S.; Hendrich, M. P.; Hooper, A. B. *Biochemistry* **2002**, *41*, 1703–1709.
(15) Lieberman, R. L.; Arciero, D. M.; Hooper, A. B.; Rosenzweig, A. C. *Biochemistry* **2001**, *40*, 5674–5681.
(16) Balatri, E.; Banci, L.; Bertini, I.; Cantini, F.; Ciofi-Baffoni, S. *Structure* **2003**, *11*, 1431–1443.
(17) Banci, L.; Bertini, I.; Calderone, V.; Ciofi-Baffoni, S.; Mangani, S.; Martinelli, M.; Palumaa, P.; Wang, S. *Proc. Natl. Acad. Sci. U.S.A.* **2006**, *103*, 8595–8600.
(18) Banci, L.; Bertini, I.; Ciofi-Baffoni, S.; Gerothanassis, I. P.; Leontari, I.; Martinelli, M.; Wang, S. *Structure* **2007**, *15*, 1132–1140.
(19) Andruzzi, L.; Nakano, M.; Nilges, M. J.; Blackburn, N. J. *J. Am. Chem. Soc.* **2005**, *127*, 16548–16558.
(20) Horng, Y. C.; Leary, S. C.; Cobine, P. A.; Young, F. B.; George, G. N.; Shoubridge, E. A.; Winge, D. R. *J. Biol. Chem.* **2005**, *280*, 34113–34122.
(21) Abriata, L. A.; Banci, L.; Bertini, I.; Ciofi-Baffoni, S.; Gkazonis, P.; Spyroulias, G. A.; Vila, A. J.; Wang, S. *Nat Chem Biol* **2008**, *4*, 599–601.
(22) Mattatall, N. R.; Jazairi, J.; Hill, B. C. *J. Biol. Chem.* **2000**, *275*, 28802–28809.
(23) Nittis, T.; George, G. N.; Winge, D. R. *J. Biol. Chem.* **2001**, *276*, 42520–42526.
(24) Chinenov, Y. V. *J. Mol. Med.* **2000**, *78*, 239–242.
(25) Ye, Q.; Imriskova-Sosova, I.; Hill, B. C.; Jia, Z. *Biochemistry* **2005**, *44*, 2934–2942.
(26) Williams, J. C.; Sue, C.; Banting, G. S.; Yang, H.; Glerum, D. M.; Hendrickson, W. A.; Schon, E. A. *J. Biol. Chem.* **2005**, *280*, 15202–15211.
(27) Siluvai, G. S.; Nakano, M.; Mayfield, M.; Nilges, M. J.; Blackburn, N. J. *Biochemistry* **2009**, *48*, 12133–12144.
(28) Blackburn, N. J.; Ralle, M.; Gomez, E.; Hill, M. G.; Patsuszyn, A.; Sanders, D.; Fee, J. A. *Biochemistry* **1999**, *38*, 7075–7084.

$CaCl_2$, 0.2% glucose, 0.05% thiamine, and 2 mL of a 50× stock of L-amino acids minus methionine, containing 50 μg/mL ampicillin and 20 μg/mL normal methionine.[29] This culture was incubated overnight at 37 °C. After the cells had begun to recover and grow in this medium, 10 mL of this culture was then transferred to 1 L of M9 enhanced minimal medium containing 20 μg/mL of SeM plus ampicillin, and growth was continued to a final OD_{600} between 0.6 and 0.8. Cultures were induced with 1 mM isopropylthio-β-D-galactoside (IPTG) for apoprotein production. The apoproteins were purified on a chitin affinity column, and the intein linker protein was cleaved with 2-mercaptoethanesulfonate (MESNA) as described previously.[19] The purified proteins were analyzed for protein concentration by Bradford assay, and their purity was checked by sodium dodecyl sulfate polyacrylamide gel electrophoresis (SDS−PAGE) on an Amersham Biosciences PHAST system (20% homogeneous gel). C45A, C49A, WT-SeM, and C45A-SeM were further analyzed by electrospray mass spectrometry and gave mass values of 19 732.3, 19 728.7, 19 850.9, and 19 855.8 Da, respectively (Figures S1−S4, Supporting Information). The wild-type (WT) protein purified by the same method gave a mass value of 19 756.6 Da (Figure S5), where the calculated mass for WT with the two cysteines present as a disulfide is 19 766.3 Da. The difference in mass values between WT and WT-SeM is 94.3 Da, corresponding to a theoretical difference between two methionine and two selenomethionine residues of 93.8 Da. Also, the difference in mass values between C45A and C45A-SeM is 93.5 Da, corresponding to two SeM residues in place of methionine. When necessary, proteins were concentrated using Amicon centricon filters of 5 kDa molecular weight cutoff (MWCO). After concentration and/or copper reconstitution (*vide infra*), protein concentrations were determined from the absorption at 280 nm using an extinction coefficient of 19 180 M^{-1} cm^{-1}.[25] Buffers used were reagent grade, and water was purified to a resistivity of 17−18 MΩ with a Barnstead Nanopure deionizing system.

General Protocol for Cu(II) Reconstitution. The purified BSco apoproteins of WT, WT-SeM, C45A, and C45A-SeM were concentrated to 100 μM in 50 mM Na-P buffer, pH 7.2. Dithiothreitol (DTT) was added to 10 mM, followed by exhaustive dialysis to remove the excess DTT. Next, 1.0 molar equiv of $CuSO_4$(aq) was added to the disulfide-reduced proteins, followed by continued anaerobic dialysis or repeated buffer exchanges using 50 mM Na-P buffer, pH 7.2, to remove non-specifically bound copper and unbound free copper in the samples. For S K-edge XAS measurements, the apoproteins were reconstituted with $Cu(NO_3)_2$(aq) to avoid interference from sulfate anion. The reconstituted proteins were concentrated to the desired concentration using Amicon centricon filters of 5 kDa MWCO. The Cu(II)-reconstituted proteins were analyzed for copper concentration using inductively coupled plasma optical emission spectrometry (ICP-OES). The C49A variant was loaded with Cu(II) via an *in situ* addition of 0.9 equiv of $CuSO_4$(aq) to the reduced apoprotein for various spectroscopic characterizations. EPR samples were prepared using $^{65}Cu(NO_3)_2$(aq) made by dissolving ^{65}CuO (Oak Ridge National Laboratory) in concentrated nitric acid.

Extinction coefficients of the unstable Cu(II) forms of C45A and C49A variants were determined by a combination of ICP-OES, EPR, and UV/vis spectroscopy. After *in situ* reconstitution of Cu(II) with 1.0 molar equiv of $Cu(SO_4)_2$ or $Cu(NO_3)_2$, the unbound Cu(II) was removed by quickly passing through a pre-equilibrated desalting spin column (Pierce). The total copper concentration was then determined by ICP-OES, and the Cu(II) concentration was determined by EPR. The extinction coefficient was then determined from the UV/vis spectrum (quick scan, 0.7 min) measured immediately after Cu(II) addition, using the EPR-determined Cu(II) concentration. This procedure resulted in an approximate error of 10% in all reported extinction values.

High-Resolution Gel Filtration Chromatography. HPLC gel filtration chromatography was performed with a Varian Prostar solvent delivery module, a Varian Prostar UV/vis detector set at 280 nm, and a Bio-Rad Bio-Sil SEC-250 (7.8 × 300 mm) gel filtration column. Typically, 5 μL of the protein samples of 100 μM concentrations were injected onto the column. Sodium phosphate (50 mM, pH 7.2) containing 500 mM NaCl was used for column equilibration and elution. Molecular weights were determined by comparison to Bio-Rad gel filtration standard number 151-1901, containing 10 mg/mL bovine thyroglobulin (670 kDa), 10 mg/mL bovine γ-globulin (158 kDa), 10 mg/mL chicken ovalbumin (44 kDa), 5 mg/mL horse myoglobin (17 kDa), and 1 mg/mL vitamin B12 (1.35 kDa).

k_{on} Rate Constant for Cu(II) Binding. The rate of Cu(II) binding was measured on an Applied Photophysics SX-18MV sequential stopped-flow spectrometer equipped with a photomultiplier (for single wavelength) and/or photodidode array at 23 °C. Typically equal volumes of disulfide-reduced apoprotein and aqueous cupric sulfate were mixed anaerobically to obtain a reaction mixture of ∼100 μM protein and 1 molar equiv of Cu(II). The reactions were monitored at the wavelengths of the maximum absorbance of the copper proteins. Absorbance changes were analyzed as a function of time by using Origin 6.0 software.

UV/Vis Spectroscopy. UV/vis spectra were collected under anaerobic conditions in septum-sealed 1 cm path-length cuvettes using a Cary 50 spectrophotometer at 23 °C. For UV/vis measurements on unstable Cys-to-Ala variants, the reduced apoproteins were reconstituted *in situ* in 50 mM sodium phosphate buffer, pH 7.2, with 1 molar equiv of $CuSO_4$(aq).

Cu K-Edge X-ray Absorption Spectroscopy. Cu K-edge (8.980 keV) extended X-ray absorption fine structure (EXAFS) and X-ray absorption near-edge structure (XANES) data for copper-substituted BSco variants were collected at the Stanford Synchrotron Radiation Lightsource, operating at 3 GeV with currents between 100 and 80 mA. Data were collected on beamline 9-3 employing a fully tuned Si(220) monochromator and a Rh-coated mirror upstream of the monochromator with a 13 keV energy cutoff to reject harmonics. A second Rh mirror downstream of the monochromator was used to focus the beam. Data were collected in fluorescence mode using a high-count-rate Canberra 30-element Ge array detector with maximum count rate below 120 kHz. A Z-1 metal oxide (Ni) filter and Soller slit assembly were placed in front of the detector to reduce the elastic scatter peak. Six scans of a sample containing only sample buffer (50 mM Na-PO_4, pH 7.2) were collected, averaged, and subtracted from the averaged data for the protein samples to remove Z-1 K_β fluorescence and produce a flat pre-edge baseline. The samples (80 μL) were measured as aqueous glasses in 20% ethylene glycol at 15 K. Energy calibration was achieved by reference to the first inflection point of a copper foil (8980.3 eV), placed between the second and third ionization chambers. Data reduction and background subtraction were performed with the program modules of EXAFSPAK.[30,31] Data from each detector channel were inspected for glitches and nonlinear events before inclusion in the final average. Spectral simulation was carried out with EXCURVE 9.2,[32−35] as previously described.[36] This allowed for inclusion of multiple scattering pathways between the metal center and the atoms of imidazole rings of histidine residues. The experimental threshold energy, E_0, was chosen as 8985 eV. The structural parameters varied during the

(29) Cutting, S. M.; Youngman, P. *Methods for General and Molecular Biology*; ASM Press: Washington, DC, 1994.

(30) George, G. N.; Stanford Synchrotron Radiation Laboratory: Menlo Park, CA, 1995.
(31) George, G. N.; Stanford Synchrotron Radiation Laboratory: Menlo Park, CA, 1990.
(32) Binsted, N.; Gurman, S. J.; Campbell, J. W.; 9.2 ed.; Daresbury Laboratory: Warrington, England, 1998.
(33) Gurman, S. J.; Binsted, N.; Ross, I. *J. Phys. C* **1984**, *17*, 143–151.
(34) Gurman, S. J.; Binsted, N.; Ross, I. *J. Phys. C* **1986**, *19*, 1845–1861.
(35) Binsted, N.; Hasnain, S. S. *J. Synchrotron Rad.* **1996**, *3*, 185–196.
(36) Blackburn, N. J.; Rhames, F. C.; Ralle, M.; Jaron, S. *J. Biol. Inorg. Chem.* **2000**, *5*, 341–353.

fitting process include the bond distance (R) and the bond variance ($2\sigma^2$), which is related to the Debye−Waller factor, resulting from thermal motion and static disorder of the absorber−scatterer pair. The nonstructural parameter, ΔE_0, was also allowed to vary but was restricted to a common value for every component in a given fit. Coordination numbers were systematically varied in the course of the fitting process.

EPR Spectroscopy. Quantitative X-band (9.4 GHz) EPR spectra were recorded on a Bruker Elexsys E500 spectrometer equipped with a Bruker ER049X SuperX microwave bridge and an E27H lock-in detector. Temperature control was provided by a continuous nitrogen flow cryostat system. Frozen Cu(II) protein samples of concentration between 100 and 500 μM in 50 mM sodium phosphate buffer at pH 7.2 were used. EPR tubes of 4 mm diameter were used for all the measurements. Spectra were collected at 90−110 K under nonsaturating power conditions, and the Cu(II) signal was doubly integrated to give the number of copper atoms per protein using Cu^{II}(EDTA) as a quantitative standard. Spectra for simulation (reconstituted with ^{65}Cu(II)) were recorded at the Illinois EPR Center on a Varian E-122 spectrometer. The samples were run as frozen glasses at ∼110 K using a continuous nitrogen flow cryostat system. Magnetic fields were calibrated with an NMR gaussmeter. Simulations were carried out using the SIMPIPM program developed at the University of Illinois.[37]

S K-Edge Spectroscopy. S K-edge data of the oxidized proteins of WT, WT-SeM, C45A, and C45A-SeM were measured using the 54-pole wiggler beamline 6-2 in high magnetic field mode of 10 kG with a Ni-coated harmonic rejection mirror and a fully tuned Si(111) double crystal monochromator. Details of the optimization of this beamline for low-energy measurements and the experimental setup have been described previously.[5,38] The protein solution was pre-equilibrated in a water-saturated He atmosphere for ∼1 h to minimize He bubble formation in the sample cell during the experiment. Protein solutions were loaded into a Pt-coated Al-block sample holder with a ∼6.35 μm thick polypropylene window using a syringe. S K-edge measurements were performed at ∼4 °C. The temperature was regulated using a cryostat, which utilizes liquid-nitrogen-cooled N_2 gas flowing through an internal channel in the sample holder. Sulfur fluorescence data were collected using an argon-filled ionization chamber as a detector. The S K-edge data presented here were averaged and processed as described previously.[5,38] Energy calibration was achieved from the S K-edge spectra of $Na_2S_2O_3 \cdot 5H_2O$ run at intervals between sample scans. The first inflection point was assigned to 2472.02 eV. A sharp sulfonate feature at 2473.4 eV (due to a small amount of residual MESNA from the protein purification) was removed by subtraction of a fraction of a pure MESNA spectrum. Copper reconstitution of C45A and C45A-SeM resulted in a net Cu(II) percentage of 65% and 31%, respectively, with the rest of the protein as Cu(I). Therefore, a correction was applied to the calculation of the percent covalency to take account of the contribution of the Cu(I) species to the total S signal during the renormalization process. No photoreduction of proteins was encountered during the measurements.

Resonance Raman Spectroscopy. Samples of Cu(II)-reconstituted WT and C45A BSco were loaded onto a multiwell sample holder mounted on a closed-cycle cryogenic system (Displex, Advanced Research Systems). The resonance Raman spectra were obtained using a backscattering geometry on a custom McPherson 2061/207 spectrograph (set at 1.0 m, 3600 groove grating) equipped with a Princeton Instruments liquid-N_2-cooled CCD detector (LN-1100PB). Kaiser optical holographic supernotch filters were used to attenuate Rayleigh scattering generated by the 413 nm excitation (140 mW power) of an Innova 302 krypton laser (Coherent, Santa Clara, CA). Absolute frequencies, accurate to at least ±1 cm^{-1}, were obtained by calibration with aspirin. The samples were stable toward laser irradiation, and Raman spectra on the same sample could be recorded for 5 h.

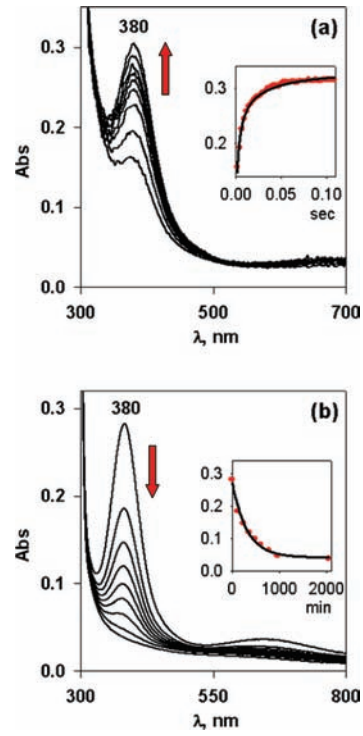

Figure 1. Formation (a) and decay (b) of the yellow Cu(II) complex (**1**) of the C49A variant of BSco. Initial concentrations of BSco and Cu(II) were 100 μM in 50 mM NaPhos buffer pH 7.2.

Results

Cu(II) Binding to C49A. When one mole equivalent of Cu(II) is added anaerobically to the thiol-reduced C49A apoprotein, it rapidly forms a yellow Cu(II) species (**1**) (Figure 1a) in a single exponential process with a pseudo first order rate constant of 79 ± 8 s^{-1} for initial Cu(II) and BSco concentrations of 100 μM. Complex **1** has an intense electronic absorption at 380 nm (ε, 3245 $M^{-1}cm^{-1}$) corresponding to a monothiolate, $RS^- \rightarrow Cu^{2+}$ CT transition and a d-d absorption centered at 640 nm (ε, 540 $M^{-1}cm^{-1}$). These absorptions are indicative of a type-2 tetragonally distorted copper site as observed earlier with various enzymatic and synthetic copper-monothiolate systems.[2,4,39−42] HPLC of **1** shows clearly that the yellow species is a monomeric form of the protein. An intermediate with maximum absorption at 380 nm was recently reported during copper loading of the WT protein[43] which may also arise from the formation of a monothiolate capture complex. The yellow C49A Cu(II) species is unstable under anaerobic conditions undergoing autoredox in a single exponential process with a half-life of 4.52 h (k = 4.26 ± 0.3 × 10^{-5} s^{-1}) to yield ∼ 45−55% of Cu(I)-C49A as end product (Figure 1b).

(37) Nilges, M. J.; *Illinois EPR Research Center (IERC)*, University of Illinois: Urbana-Champaign, 1979.
(38) Hedman, B.; Frank, P.; Gheller, S. F.; Roe, A. L.; Newton, W. E.; Hodgson, K. O. *J. Am. Chem. Soc.* **2002**, *110*, 3798–3805.
(39) van Amsterdam, I. M.; Ubbink, M.; van den Bosch, M.; Rotsaert, F.; Sanders-Loehr, J.; Canters, G. W. *J. Biol. Chem.* **2002**, *277*, 44121–44130.
(40) Han, J.; Loehr, T. M.; Lu, Y.; Valentine, J. S.; Averill, B. A.; Sanders-Loehr, J. *J. Am. Chem. Soc.* **1993**, *115*, 4256–4263.
(41) Lu, Y.; Roe, J. A.; Bender, C. J.; Peisach, J.; Banci, L.; Bertini, I.; Gralla, E. B.; Valentine, J. S. *Inorg. Chem.* **1996**, *35*, 1692–1700.
(42) Mandal, S.; Das, G.; Singh, R.; Shukla, R.; Bharadwaj, P. K. *Coord. Chem. Rev.* **1997**, *160*, 191–235.
(43) Cawthorn, T. R.; Poulsen, B. E.; Davidson, D. E.; Andrews, D.; Hill, B. C. *Biochemistry* **2009**, *48*, 4448–4454.

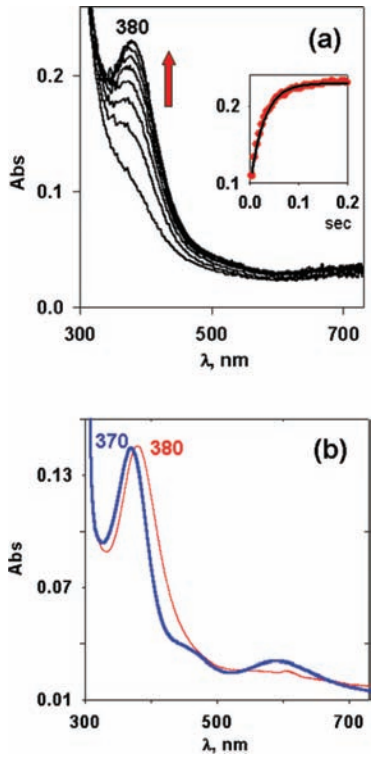

Figure 2. (a) Formation of the Cu(II) complex of C45A BSco monitored by stopped flow. (b) subsequent rearrangement of the yellow complex initially formed (**2**) with λ_{max} = 380 nm to the stable green complex (**3**) with λ_{max} = 370 nm. The initial concentration of BSco and Cu(II) were 100 μM in 50 mM NaPhos buffer pH 7.2.

Cu(II) Binding to C45A. Like the C49A variant, C45A also forms a yellow species (**2**) upon anaerobic addition of Cu(II) (pseudo first order rate constant of 35 ± 5 s^{-1} for initial [Cu(II] and [BSco] = 100 μM) with a characteristic absorption at λ_{max} 380 nm (ε, 2310 ± 200 $M^{-1}cm^{-1}$) (Figure 2a). As shown in Figure 2(b), **2** is unstable and converts into a stable green Cu(II) species, Cu(II)-C45A (**3**) having electronic absorption features at 370 nm (2650 ± 200 $M^{-1}cm^{-1}$), 455 nm (430 ± 50 $M^{-1}cm^{-1}$), and 600 nm (410 ± 50 $M^{-1}cm^{-1}$) (Figure 2b).

The time course of this conversion is complex, but initially involves a moderately rapid decomposition of **2** as measured by the decrease in absorption at 400−450 nm which proceeds with a half-life of 1.5 min. However, full conversion to the green species takes approximately one hour to complete. Quantitation of the Cu(II) spin from X-band EPR together with the concentration of copper from ICP-OES reveals the existence of ∼65% copper in complex **3** as Cu(II) and the rest as Cu(I). Similar Cu(II) incorporation chemistry was observed earlier in the double azurin variant H117G/N42C[39] and the intermediate formed when Cu(II) is added to apo Cu_A-azurin.[44]

X-ray Absorption of Cu(I) Variants. Cu(I)-bound forms of C49A and C45A variants were obtained by reconstitution of apoprotein samples with Cu(I) by methods described previously.[19,45] The XAS of Cu(I)-C49A measured at the Cu K-edge is shown in Figure 3(a). The sharp, intense feature at 8983 eV is assigned to a 1s → 4p transition in a linear two coordinated environment.[45–47]

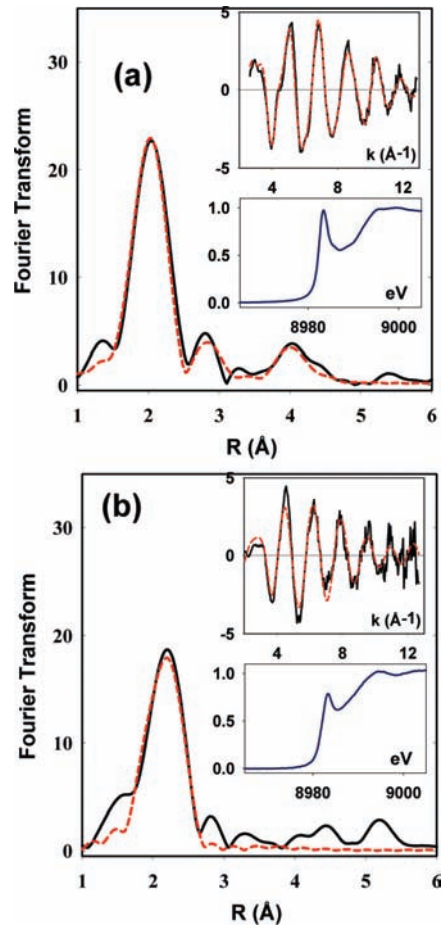

Figure 3. X-ray absorption spectra (Fourier transforms, EXAFS (top inset) and absorption edges (bottom inset)) of the Cu(I) forms of the Cys to Ala variants of BSco. (a) The C49A showing the intense 1s−$4p_{x,y}$ edge transition typical of two-coordinate species; (b) C45A showing an attenuated 1s−4p transition typical of three-coordination. Black traces are experimental data, red traces are simulated data using the parameters listed in Table 1. The Cu(I) concentrations were 1.3 and 0.75 mM for the C49A and C45A variants, respectively, in 50 mM sodium phosphate buffer, pH 7.2.

Fits to S_{Cys} and N_{His} ligand scatterers with typically short bond distances of Cu−S = 2.12 Å and Cu−N = 1.88 Å further support the two coordinated structure.[45,48,49] In fact, this is the first linear protein structure of a cysteine plus histidine combination known so far in copper protein chemistry, although two coordinated structures of Cu(I) with two cysteines are common, for example in ATX-like proteins and domains such as the copper chaperone HAH1 and its target, Menkes protein (N-MNKp).[45,49,50]

X-ray absorption spectra of the Cu(I)-reconstituted C45A derivative are shown in Figure 3(b). The data show significant differences to those of the C49A variant. Specifically, the absorption edge feature at 8983 eV is of lower intensity, which implies either two-coordination with a strong distortion from linearity or a 3-coordinate environment. Initial fits explored combinations of scattering atoms consisting of one S(Cys) and

(44) Wang, X.; Ang, M. C.; Lu, Y. *J. Am. Chem. Soc.* **1999**, *121*, 2947–2948.
(45) Ralle, M.; Lutsenko, S.; Blackburn, N. J. *J. Biol. Chem.* **2003**, *278*, 23163–23170.
(46) Pickering, I. J.; George, G. N.; Dameron, C. T.; Kurz, B.; Winge, D. R.; Dance, I. G. *J. Am. Chem. Soc.* **1993**, *115*, 9498–9505.
(47) Kau, L. S.; Spira-Solomon, D.; Penner-Hahn, J. E.; Hodgson, K. O.; Solomon, E. I. *J. Am. Chem. Soc.* **1987**, *109*, 6433–6422.
(48) Himes, R. A.; Park, Y. G.; Barry, A. N.; Blackburn, N. J.; Karlin, K. D. *J. Am. Chem. Soc.* **2007**, *129*, 5352–5353.
(49) Chen, K.; Yuldasheva, S.; Penner-Hahn, J. E.; O'Halloran, T. V. *J. Am. Chem. Soc.* **2003**, *125*, 12088–12089.
(50) Ralle, M.; Cooper, M. J.; Lutsenko, S.; Blackburn, N. J. *J. Am. Chem. Soc.* **1998**, *120*, 13525–13526.

Table 1. Parameters Used in the Fits to the EXAFS Data of the Cu(I) and Cu(II) Forms of the C49A and C45A Variants of BSco

		Cu−N(Histidine)[c]			Cu−O/N			Cu−S(Cys)			
Sample	F[a]	No.[b]	Distance (Å)[d]	Debye−Waller (Å²)[e]	No.[b]	Distance (Å)[d]	Debye−Waller (Å²)[e]	No.[b]	Distance (Å)[d]	Debye−Waller (Å²)[e]	$-\Delta E_0$
Cu(I)-C49A	0.257	1 N1	1.88	0.005				1	2.12	0.005	1.01
		1 C2	2.89	0.006							
		1 C5	2.89	0.006							
		1 C3	4.01	0.013							
		1 N4	4.05	0.013							
Cu(II)-C49A	0.218	2 N1	1.93	0.011	1	2.09	0.008	1	2.15	0.010	
		2 C2	3.00	0.014							
		2 C5	2.86	0.014							
		2 C3	4.14	0.028							
		2 N4	4.03	0.028							
Cu(I)-C45A	1.085	1 N	2.05	0.015				2	2.28	0.017	9.91
Cu(II)-C45A	0.341	2 N1	1.92	0.012	1	2.06	0.008	1	2.15	0.010	2.58
		2 C2	2.97	0.020							
		2 C5	2.90	0.020							
		2 C3	4.17	0.020							
		2 N4	4.04	0.020							

[a] F is a least-squares fitting parameter defined as $F^2 = (1)/(N)\sum_{i=1}^{N} k^6(Data - Model)^2$ [b] Coordination numbers are generally considered accurate to ± 25% [c] Fits modeled histidine coordination by an imidazole ring, which included single and multiple scattering contributions from the second shell (C2/C5) and third shell (C3/N4) atoms respectively. The Cu−N−C_x angles were as follows: Cu−N−C2 126°, Cu−N−C3 −126°, Cu−N−N4 163°, Cu−N−C5 −163°. [d] In any one fit, the statistical error in bond-lengths is ± 0.005 Å. However, when errors due to imperfect background subtraction, phase-shift calculations, and noise in the data are compounded, the actual error is probably closer to ± 0.02 Å. [e] Debye−Waller factors are quoted as $2\sigma^2$ values.

one or more O/N ligands, where the N shell was simulated either with or without the multiple scattering contributions expected from the outer-shell C and N atoms of imidazole (histidine) ligation. These fits showed a strong preference for a 2-coordinate structure but with chemically unreasonable Cu−S distance of 2.29 Å. Two-coordinate Cu−S distances are expected to be in the range 2.13−2.18 Å[45,49–51] whereas longer distances 2.25−2.30 Å are typical for 3-coordination.[46] Fits with comparable F values could be obtained by increasing the Cu−S or Cu−O/N shell from one to two, but this was at the expense of unreasonably high Debye−Waller factors (Table 1). In all cases the fits discriminated against the inclusion of imidazole outer-shell scattering. Therefore, the coordination environment of the Cu(I)-C45A species is not clearly defined by EXAFS, and may represent a mixture of species with different coordination numbers and/or bond lengths.

EPR of Cu(II) Forms. As discussed above, Cu(II) forms of the Cys to Ala variants initially form a similar yellow species on addition of Cu(II) but undergo further reaction to form in the case of C45A, a modified stable green species (**3**) or in the case of C49A a Cu(I) product as the result of autoredox reactivity. To probe the Cu(II) species further we measured EPR spectra at X-band frequencies. Samples of the C45A species **3** were prepared by allowing the Cu(II) reconstituted apoprotein to convert to the green form over a period of 2 h. This resulted in a stable species integrating to 65% Cu(II) and 35% Cu(I), the latter component most likely resulting from competing autoreduction of the initial yellow intermediate. For C49A the prediction was that the Cu(II)-C49A species could be trapped by freezing immediately after copper addition, and samples prepared in this way integrated to 85 ± 5% Cu(II). Figure 4(a) and (b) show the X-band EPR spectra of the C45A stable green species **3**, and the C49A trapped Cu(II) species respectively. The spectra were simulated using the program SIMPIPM and selected spin Hamiltonian parameters derived from the simulations are given in Table 2. The C45A spectrum can be fit to a single species, while the C49A data require the presence of two components, - a sharp component with resolved ^{14}N hyperfine present at 40% occupancy and a broad component present at 60% occupancy (component spectra are shown in Figure S7 of the Supporting Information). The spectra differ significantly from the WT with the most notable difference being the value of g_z which increases from 2.15 to 2.18 in C45A and to 2.23 (sharp)/2.25(broad) in C49A. While these changes in g_z certainly reflect the loss of one cysteine residue, they also indicate a marked difference in the electronic properties of the two variants with C45A having a more covalent character than C49A. Of additional interest, the C45A spectra show a resolved 5-line superhyperfine pattern on the two low-field parallel copper hyperfine lines which simulates to two nearly equivalent nuclei with nuclear spin = 1, assignable to ^{14}N superhyperfine coupling. Coupling to one N from histidine was previously detected in the WT X-band CW spectra, and in the ENDOR, and assigned to coordination of His135.[19] It is likely that one of the Ns in C45A spectra can also be assigned to H135. The origin of the second N coupling is less clear, but the near equivalence of the coupling suggests His55 as the most likely candidate. This is the only other His residue in the sequence and was previously found to be broadened in the NMR of the WT protein.[16] The anisotropic part of the two^{14}N hyperfine matrices are both oriented in the same direction, implying not only that the two nitrogen's are trans to each other but that Cys 45 is trans to His 135. This is also consistent with our earlier observation[27] that the Cys 45 and 49 are oriented cis to each other. Unlike WT, EPR measurements of C45A exchanged in D_2O, showed no decrease in line width, implying that there is no nearby exchangeable proton.

The EPR of the trapped C49A Cu(II) species is more complex. The g_z = 2.23 value for the narrow species is indicative of a less covalent species with less delocalization of spin away from copper onto the S ligand. Unlike C45A, the spectra can be simulated by a single N coupling, again suggesting a decrease in electronic coupling to ligand nuclei,

(51) Pufahl, R. A.; Singer, C. P.; Peariso, K. L.; Lin, S.-J.; Schmidt, P. J.; Fahrni, C. J.; Cizewski Culotta, V.; Penner Hahn, J. E.; O'Halloran, T. V. *Science* **1997**, *278*, 853–856.

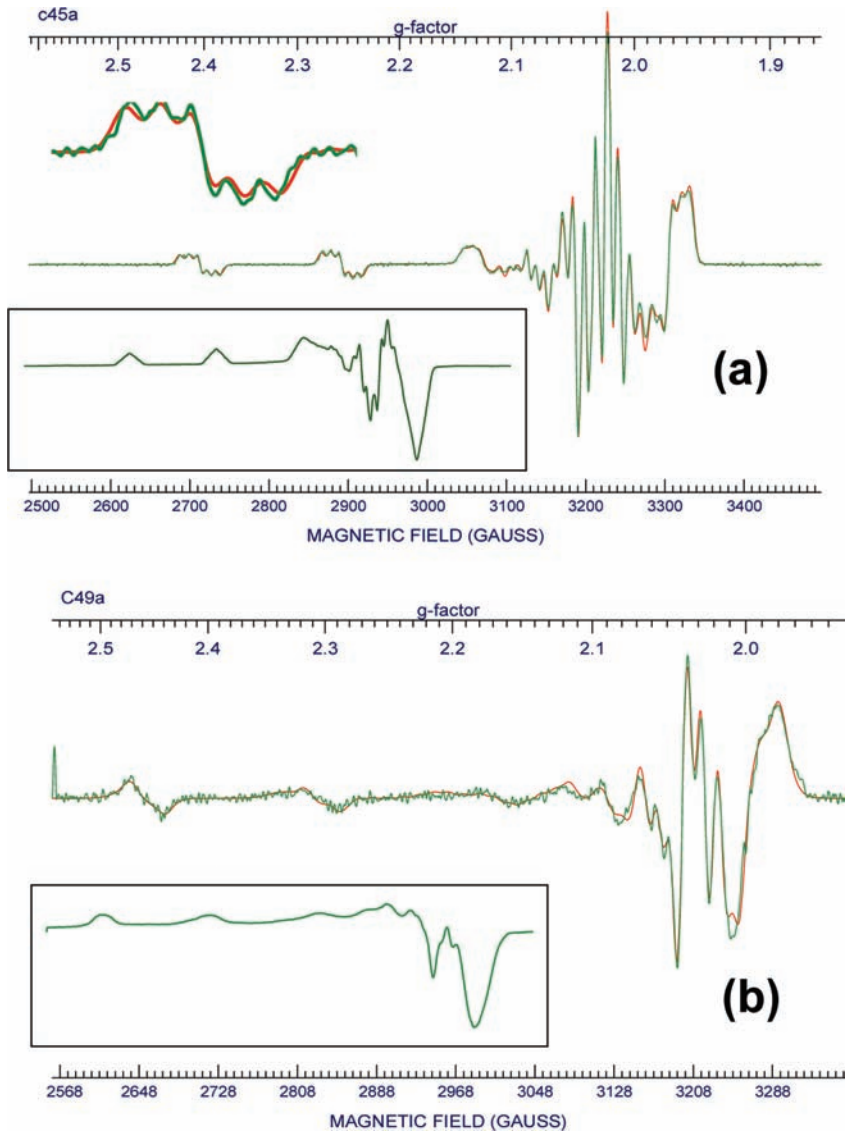

Figure 4. CW X-band EPR spectra for (a) C45A and (b) C49A variants of BSco. Spectra are plotted as second derivatives with the first-derivative spectra shown as insets at reduced scale. Green lines are experimental data, red lines are simulated data using the parameters listed in Table 2. The experimental parameters are: center field 3050 G, sweep width 800 G, modulation amplitude 2G, modulation frequency 100 kHz, number of scans 30, temperature 110 K, microwave power 1.0 mW, microwave frequency ~ 9.12 GHz.

Table 2. Selected Spin Hamiltonian Parameters Used in the Simulation of CW EPR Spectra of BSco Cysteine to Alanine Variants[a]

	Wild Type[b]	C45A	C49A (sharp species)	C49A (broad species)
g_x	2.0342(3)	2.0496(3)	2.0583(4)	2.0361(8)
g_y	2.0288(3)	2.0281(3)	2.0350(4)	2.0647(8)
g_z	2.1503(3)	2.1876(3)	2.2311(4)	2.2543(8)
$A_x(^{65}Cu)$	−135(2)	−105(2)	−109(3)	−84(8)
$A_y(^{65}Cu)$	−115(2)	−72(2)	−65(3)	−51(8)
$A_z(^{65}Cu)$	−572(2)	−549(2)	−554(3)	−512(8)
$N1(A_x)$	30 (1)	30(1)	33(2)	
$N1(A_y)$	41(1)	39(1)	45(2)	
$N1(A_z)$	31(1)	34(1)	38(2)	
$N2(A_x)$		27(1)		
$N2(A_y)$		36(1)		
$N2(A_z)$		29(1)		
$H(A_x)$	21(3)	12(3)	9(3)	
$H(A_y)$	16(3)	15(3)	12(3)	
$H(A_z)$	18(3)	12(3)	18(3)	

[a] Hyperfine principal values in MHz (For units of 10^{-4} cm^{-1}, divide by 3). For equivalent ^{63}Cu hyperfine values, use $A(^{63}Cu) = A(^{65}Cu)/1.0713$. Estimated error values given in parentheses. [b] Reference 27.

and a significantly different electronic environment of the copper center. It is also interesting to note that all three principal values of g are nearly identical to those of nitrosocyanin,[5] suggesting that the structure of the C49A Cu(II) species is similar in ways to that in nitrosocyanin. However, the structures do differ as indicated in the larger copper hyperfine coupling for C49A. The nature of the broad species is unclear.

XAS of Cu(II)-Bound Variants. XAS offers an additional approach to comparing the coordination environments of the C45A and C49A variants. Because of the autoredox reactions observed for both variants, it was first necessary to assess the extent of photoreduction in the X-ray beam. This was achieved by exposing samples prepared by the same protocol as for EPR to a minimum dose of radiation while performing a succession of rapid scans through the absorption edge each taking 100 s, using computer control to close the shutter during the monochromator movement and settling time. For these experiments, the beam flux was attenuated 10-fold by inserting an Al filter in front of the I_0 ionization chamber. Figure 5(a) and (b) show

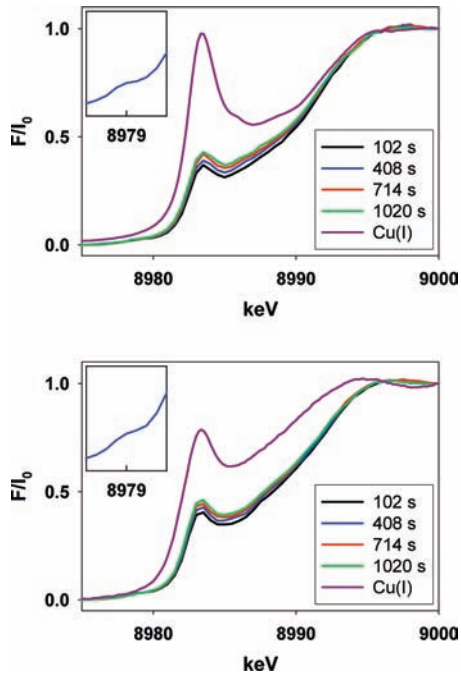

Figure 5. Stability of the Cys to Ala variants with respect to photoreduction. The figure compares the absorption edges of the Cu(II) derivative measured at 100 s intervals with that of the stable Cu(I) form. C49A data are shown in the top panel while C45A data are shown in the bottom panel. Samples were exposed to the minimum dose of radiation while performing a succession of rapid scans through the absorption edge each taking 100 s, using computer control to close the shutter during the monochromator movement and settling time. The beam flux was attenuated 10-fold by inserting an Al filter in front of the I_0 ionization chamber. The top (purple) spectrum in each panel is the fully reduced protein formed by reconstitution of apoprotein with Cu(I).

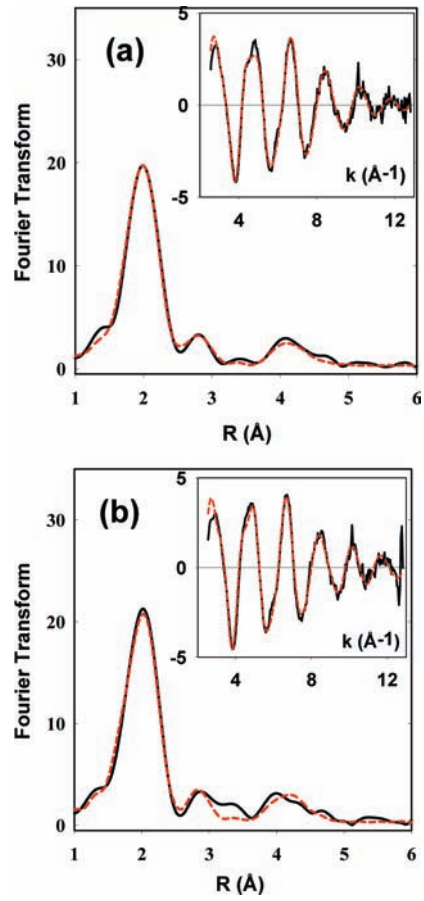

Figure 6. Fourier transforms and EXAFS (inset) for the Cu(II) forms of (a) C45A and (b) C49A variants of BSco. Parameters used to generate the fits are listed in Table 1. Cu(II) concentrations were 1.6 and 2.5 mM respectively.

the results for the two Cys to Ala variants. Each shows almost identical absorption edge spectra, with a weak shoulder at 8979 due to the 1s → 3d quadrupolar transition, and a more intense feature at 8983 eV which is of lower intensity than that of the fully reduced protein. Since EPR spectroscopy shows that both samples are semi-reduced (*vide supra*), the 8983 eV band is likely due to a 1s → $4p_z$ transition of the Cu(I) component.[47] However, the intensity of this peak does not increase by more than 10% during 1000 s of exposure, suggesting that this represents the level of reduction present in the samples before beam exposure.

Next a new spot was chosen, and a number of complete EXAFS scans were collected using the unattenuated beam and normal scan times (25 min). The edges of consecutive scans were compared with those determined by the initial rapid scanning and found to be identical. Therefore, the EXAFS data represents a mixture of Cu(II) and Cu(I) which we estimate from EPR to be ~65:35 for C45A and ~85:15 for C49A. EXAFS analysis provides only the average coordination and generally is poorly adapted for analysis of mixtures. Therefore EXAFS analysis in the present case is only expected to give approximations to the coordination environment. Notwithstanding, data for C45A clearly show the presence of the characteristic beat pattern between $k = 3-6$ Å^{-1} assignable to imidazole outer shell scattering. The data fit well to a 4-coordinate site comprised of two N(His), one S(Cys), and one non-His O/N (Figure 6a, Table 1). This is consistent with the EPR data which show superhyperfine coupling from two nearly equivalent N atoms. Surprisingly, the C49A EXAFS data are almost identical to C45A, and can be simulated by the same parameters (Figure 6b). This suggests that the ligand set may be identical in the two variants, but the electronic structure, and localization of the unpaired spin is different. However, these results need to be interpreted with caution, given the EPR evidence for multiple speciation.

S K-Edge Spectroscopy. In copper−thiolate proteins, the extent of covalency of the copper−thiolate bond dictates the overall reactivity of the protein. The thiolate ligand has three valence 3p orbitals, one of which is greatly stabilized in energy due to the C−S σ bond and therefore does not contribute to the Cu−S bond. The two remaining 3p orbitals, which are perpendicular to the C−S bond, dominate the thiolate interaction with copper. The 3p orbital out of the C−S−Cu plane is involved in π bonding, while the in-plane 3p orbital bond to copper in a pseudo-σ fashion. A direct experimental probe of the covalency of the thiolate S−Cu bond is sulfur K-edge XAS.[13] This involves a pre-edge transition from the sulfur 1s orbital to the half-occupied molecular orbital (HOMO) ~2469 eV, contributed solely by the sulfur atoms which are covalently linked to copper. Hence, the intensity of this pre-edge transition directly reflects the sulfur 3p character mixed into the $d_{x^2-y^2}$ orbital due to covalent bonding. The rising edge corresponding to the 1s → 3p transition of sulfur is contributed by all the sulfur atoms present in the protein. Therefore, the S K-edge spectra are normalized at ~ 2490 eV and then renormalized with respect to the number of sulfur atoms in the standard, plastocyanin in order to quantify covalency. Renormalization involves multiplying the intensity of the pre-edge feature by a factor equal to the

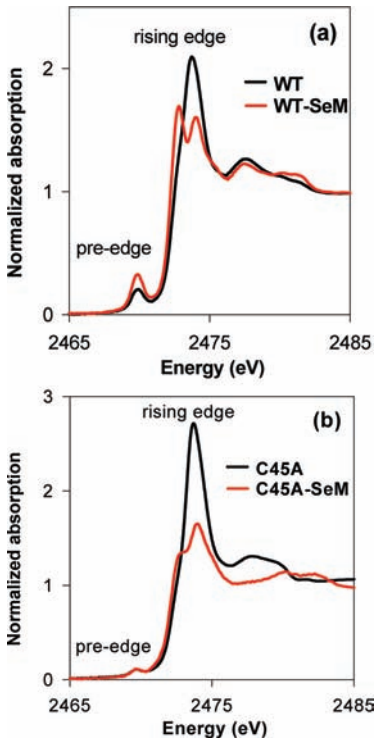

Figure 7. S K-edge spectroscopy of the Cu(II) forms of WT BSco (top) and the C45A variant (bottom). Spectra for the selenomethionine substituted forms are shown in red for comparison to eliminate the contribution due to M52 and M56 noncoordinating residues and provide an experimental check on renormalization protocols. The Cu(II) concentrations were as follows: WT Cu(II)-BSco ~ 5.4 mM; WT-SeM Cu(II)-BSco ~ 4.8 mM; C45A Cu(II)-BSco ~ 4.5 mM; C45A-SeM Cu(II)-BSco ~ 2.5 mM. The buffer was 50 mM Na Phos, pH 7.2. Spectra were measured in aqueous solution at 4 °C.

total number of S atoms in the protein. For Cu(II) centers coordinated by a single thiolate ligand such as plastocyanin or nitrosocyanin this procedure results in an estimation of the pre-edge intensity for a single Cu−S bond. However, when two thiolate ligands coordinate as is the case for BSco, the pre-edge intensity must be multiplied by two after renormalization to obtain the average covalency resulting from both Cu−S bonds. In a parallel approach we eliminated the contribution of non-coordinating methionine residues at the rising edge by mutating the two methionine residues 52 and 56 to selenomethionine and determined the S K-edge spectra for the diselenomet derivatives. Comparison of the average value of the covalency of native and diselenomet proteins should provide a check on the consistency of the renormalization procedure.

The normalized S K-edge XAS spectrum of WT and its diselenomethionine (SeM) derivative is shown in Figure 7a. The spectra showed a well-defined pre-edge feature at 2470.0 eV arising from the S(1s) → ψ^*_{HOMO} transition and a rising edge feature at 2472.8 eV due to sulfur 1s → 3p transition. The WT and WT-SeM show the expected trend, with the pre-edge increasing in intensity for the SeM derivative. Quantitation of the renormalized S K-edge pre-edge feature gives 28 and 22% sulfur character in the HOMO for the WT and WT-SeM, respectively, or an average of 14 and 11% for each of the two Cu−S bonds in WT and WT-SeM proteins respectively. The pre-edge transition for plastocyanin, nitrosocyanin and BSco occurs at 2469.0, 2469.7, and 2470.0 eV, respectively and the rising edge transition occurs at 2473.5, 2473.0, and 2472.8 eV, respectively.[5] These data illustrate the trend in the energy of the HOMO which increases throughout the series plastocyanin to nitrosocyanin to BSco, which may be attributed to an increase in the ligand field consistent with an increased effective coordination number. The spectra of the C45A variant showed a well-defined pre-edge feature at 2469.7 eV and a rising edge feature at 2472.6 eV (Figure 7b). Quantitation of the renormalized S K-edge pre-edge feature gives 8.5 and 4.4% covalency for the single Cu−S bond in C45A and C45A-SeM, respectively. The presence of Cu(I) in these samples due to autoredox reactions, coupled to imprecision in estimating the Cu(I)/Cu(II) ratios make these latter values less reliable, and the larger observed differences between S(Met) and SeM derivatives is likely due to similar factors.[52]

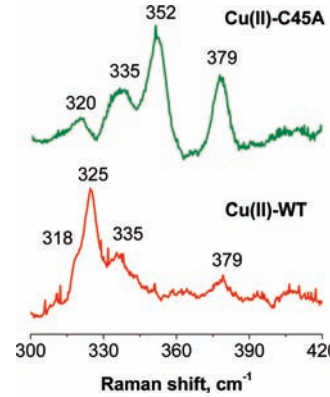

Figure 8. Resonance Raman spectra of Cu(II)-WT ($\langle\nu_{Cu-S}\rangle = 326\ cm^{-1}$) and Cu(II)-C45A ($\langle\nu_{Cu-S}\rangle = 353\ cm^{-1}$) BSco with excitation energy at 413 nm. Spectra were measured at 30 K using an output power 140 mW.

Resonance Raman Spectroscopy of the Cu(II) Proteins of WT and C45A. RR spectra reflect the copper cysteine sulfur bond strength and hence we measured and compared the resonance Raman spectra of WT and C45A Cu(II) proteins to identify the vibrational contributions from the two cysteine thiolates.[3,4] Excitation into the $S_{Cys} \rightarrow Cu^{2+}$ CT transitions at 413 nm yields three fundamental vibrations for the WT with a strongest stretching vibration at 325 cm^{-1} and four fundamental vibrations for the C45A variant with a strongest stretching vibration at 352 cm^{-1}, in the 310−380 cm^{-1} region associated with vibrations containing the Cu−S distortion (Figure 8). The large number of frequencies observed for the C45A variant compared to the single mode predicted for an isolated Cu−S center has been ascribed to vibronic and kinematic coupling of the Cu−S stretch (ν_{Cu-S}) with cysteine ligand deformations and cysteine modes of similar energy (δ_{Cys}).[53−56] The Cu−S

(52) An additional factor which must be taken into consideration when comparing the S-K edge data with results from other spectroscopy is a possible difference induced by measuring the data at different temperatures. Due to experimental considerations the S-K edge data were measured at 4 °C rather than the low temperature (10−110 K) used for EXAFS, EPR and resonance Raman data. Phosphate buffers are known to shift downwards in pH by up to 2 pH units upon freezing to 77 K, due to the insolubility of the dibasic salt at low temperature (see: Williams-Smith, D. L.; Bray, R. C.; Barber, M. J.; Tsopanakis, A. D.; Vincent, S. P. *Biochem. J.* **1977**, *167*, 593–600). Therefore we measured the pH dependence of the UV/vis spectrum of the WT BSco from pH 2 to pH 10. Only very minor differences in extinction were observed between pH 7 and pH 2, indicating that the structure of the Cu(II) site remains essentially unchanged over this pH range. A plot of the UV/vis spectrum of BSco vs pH is shown as Supporting Information Figure S8.

(53) Han, J.; Adman, E. T.; Beppu, T.; Codd, R.; Freeman, H. C.; Huq, L.; Loehr, T. M.; Sanders-Loehr, J. *Biochemistry* **1991**, *30*, 10904–10913.

vibrations of BSco proteins appear in the same region as that of the variants of SOD and azurin (Table 4, below). The intensity-weighted average stretching frequency ($<\nu_{Cu-S}> = \sum_i(I_i\nu_i^2)/\sum_i(I_i\nu_i)$) of the WT protein is 326 cm^{-1} and that of the C45A variant protein is 353 cm^{-1}.[57] Thus, the average Cu−S bond strength increases in the variant, which is expected on account of the loss of one of the coordinating Cys residues. From the average stretching frequency, the bond length of the copper sulfur bond relative to a standard protein can be derived from Badger's rule: $(r_1 - d_{ij})/(r_2 - d_{ij}) = (\nu_2/\nu_1)^{2/3}$, where dij was fixed at 1.5 for first row transition metal ions.[57] By applying Badger's rule, the calculated Cu−S bond distance for the WT protein relative to nitrosocyanin ($\nu_2 = 321$ cm^{-1} and $r_2 = 2.26$ Å) is 2.24 Å while that of the C45A variant is 2.16 Å.[5] These bond lengths fit well with those derived from simulation of the EXAFS of WT (2.21 Å,[19]) and C45A (2.15 Å).

Cys to His Variants. The C45H and C49H variants were also constructed and studied to determine whether their properties resembled those of cupredoxins which exhibit a similar His_2Cys ligand donor set. These variants were unstable and like C49A underwent autoredox reactions to form colorless (presumably Cu(I)) derivatives. EXAFS data for the Cu(II) derivative of C45H were consistent with the expected N_2S coordination with Cu−N and Cu−S bond lengths of 1.93 and 2.18 Å respectively. EXAFS data for C49A showed a markedly lower Cu−S interaction corresponding to less than 0.5 Cu−S per protein, suggesting a further rearrangement in which the remaining cysteine residue was displaced in a significant fraction of molecules. EPR spectra were broad and suggestive of a multicomponent system for both derivatives. Due to the complex spectral signatures coupled with redox instability, these variants were not subjected to further study. UV/vis, EXAFS and EPR data for the Cys to His variants are presented in Figures S9−S11, while parameters used to simulate the EXAFS are given in Table S1.

Discussion

Wild type Sco proteins can be classified as "red" copper proteins on the basis of their electronic absorption spectra with λ_{max} (ε) at 354 (6400), 450 (1385), 545 (865). The UV/vis spectrum is typical of a tetragonally distorted site where the Sp_σ transition (354 nm) is more intense than the Sp_π, and occurs at higher energy.[4,5,12,14,15,58,59] The high energy Sp_σ interaction is dominant in tetragonal Cu(II)-thiolates such as tet-b and analogous complexes, and occurs around 360−370 nm with extinctions of ~5000 $M^{-1}cm^{-1}$,[58,59] with weaker $Sp_\pi \rightarrow$ Cu(II) transitions to lower energy. Here, the $d_{x^2-y^2}$ orbital is oriented in the equatorial plane, and is able to form strong σ-bonding interaction(s) with the thiolate ligands. The closest analogue of Cu(II) Sco is nitrosocyanin, the red cupredoxin protein from *Nitrosomonas europaea* which exhibits bands at 390, 496, and 720 of similar intensity to those in BSco,[5,14,15] where the Cu(II) site is best described as a square pyramid with 1 Cys, 2 His and a water in the basal plane and a carboxylate O from Glu in an axial position. Detailed electronic structural analysis[5] has assigned the 390 and 496 nm bands to the Cu−Sp_σ and Cu−Sp_π components respectively. These systems differ significantly from "blue" copper proteins which are characterized by a trigonal planar triad of one Cys and two His ligands, and a weak axial ligand at a longer distance.[1,11,12,60] Blue copper proteins exhibit the strong $Sp_\pi \rightarrow$ Cu(II) band around 600 nm and have much weaker $Sp_\sigma \rightarrow$ Cu(II) absorption around 400 nm which arise from orientation of the $d_{x^2-y^2}$ orbital in a fashion such that it now forms a strong π-interaction with a S p-orbital.[1,11,12,60] As the ligand-field of the axial ligand increases, as is the case in nitrite reductase[6] and M121X variants of azurin,[61,62] an intermediate situation is encountered: the $d_{x^2-y^2}$ rotates so as to form a more favorable sigma overlap with the S(Cys) p orbital resulting in an increase in both the Cu−S bond length and in the intensity of the 400 nm p_σ transition with a corresponding decrease in the intensity as the 600 nm p_π transition. Therefore copper proteins can be distinguished electronically by the ratio of their extinction coefficients at 400 and 600 nm.

The chemistry of cupredoxins has been largely ascribed to the uniqueness of the cupredoxin fold which pre-forms the copper binding site in a rigid protein matrix allowing only minor perturbations to the coordinate structure. It is therefore of interest to address the question of whether similar chemistry and spectroscopy is observed in other protein scaffolds. The BSco system provides an opportunity to explore these questions via site-directed mutagenesis of the thiolate ligands, thereby creating a site close to that found in cupredoxins. In the present paper, we report on two cysteine variants of BSco in which the copper−thiolate ligands C45 and C49 were individually changed to alanine and compared with the WT protein with respect to their copper-binding, reactivity, and covalency. One of these mutants C45A showed a weak resemblance to the properties of other type1 systems such as the green nitrite reductase, while the other C49A was unstable, and underwent facile autoreduction to a Cu(I) form.

Both the cysteine variants bind Cu(II) involving the initial formation of a yellow transient intermediate with $\lambda_{max} = 380$ nm. This species is similar to that described earlier in the double azurin variant H117G/N42C[39] and the intermediate formed when Cu(II) is added to apo Cu_A-azurin.[44] In the case of the H117G/N42C azurin variant it was proposed that the surface bound Cys^{42} residue initially bound Cu(II) to form a yellow species (λ_{max} 385 nm) within 10 ms after mixing believed to represent a transient involved in initial copper capture. Thereafter the system rearranges allowing Cys^{42} to enter the Cu binding cavity and form a Cu(II)-$(Cys)_2$(His) species with almost identical UV/vis spectral features. The engineered azurin containing a Cu_A binuclear binding site was found to form a similar yellow tetragonal intermediate (λ_{max} 385 nm) suggested to arise from Cu(II) capture by a Cys and a His from one-half of the Cu_A binding site. It is reasonable to suggest that the yellow intermediate formed when Cu(II) is added to either of the Sco Cys to Ala variants may be an analogous initial capture complex

(54) Dave, B. C.; Germanas, J. P.; Czernuszewicz, R. S. *J. Am. Chem. Soc.* **1993**, *115*, 12175–12176.
(55) den Blaauwen, T.; Hoitink, C. W. G.; Canters, G. W.; Ham, J.; Loehr, T. M.; Sanders-Loehr, J. *Biochemistry* **1993**, *32*, 12455–12464.
(56) Anemueller, S.; Bill, E.; Schaefer, G.; Trautwein, A. X.; Teixeira, M. *Eur. J. Biochem.* **1992**, *210*, 133–138.
(57) Blair, D. F.; Campbell, D. W.; Schoonover, D. R.; Chan, S. I.; Gray, H. B.; Malmstrom, B. G.; Pecht, I.; Swanson, B. I.; Woodruff, W. H.; Cho, W. K.; English, A. M.; Fry, H. A.; Lum, V.; Norton, K. A. *J. Am. Chem. Soc.* **1985**, *107*, 5755–5766.
(58) John, E.; Bharadwaj, P. K.; Potenza, J. A.; Schugar, H. J. *Inorg. Chem.* **1986**, *25*, 3065–3069.
(59) Stibrany, R. T.; Fikar, R.; Brader, M.; Potenza, M. N.; Potenza, J. A.; Schugar, H. J. *Inorg. Chem.* **2002**, *41*, 5203–5215.
(60) Penfield, K. W.; Gewirth, A. A.; Solomon, E. I. *J. Am. Chem. Soc.* **1985**, *107*, 4519–4529.
(61) Karlsson, B. G.; Tsai, L. C.; Nar, H.; Sanders-Loehr, J.; Bonander, N.; Langer, V.; Sjolin, L. *Biochemistry* **1997**, *36*, 4089–4095.
(62) Kroes, S. J.; Salgado, J.; Parigi, G.; Luchinat, C.; Canters, G. W. *J. Inorg. Biol. Chem.* **1996**, *1*, 551–559.

Table 3. Comparison of the Covalency and Cu−S(Cys) Bond Lengths in Mononuclear Copper−Thiolate Proteins

Sample	No. of Cys residues	Cu−S distance (Å)	Percent Covalency	ref
Wt BSco (red)[a]	2	2.28, 2.15[a]	28[b]	This work
C45A-BSco (green)[a]	1	2.14	8	This work
Nitrosocyanin (red)[b]	1	2.26	20	5
Plastocyanin (blue)	1	2.06	38	9
Nitrite reductase (green)	1	2.16	28	6
Tet-b (model)	1	2.36	15	9

[a] Individual distances are derived from an EXAFS fitting protocol which allowed the Cu−S shell to split during refinement. It should be noted that the observed splitting of 0.13 Å is equal or less than the calculated resolution of the data and may therefore be unreliable. [19] [b] The value given is the total Cu−S covalency for both Cu−S bonds.

perhaps involving the remaining Cys ligand, His135 and two other O/N ligands probably solvent. Interestingly, a similar transient has recently been reported as an intermediate in the metalation of the WT BSco, appearing as the first observable spectral species in a Cu(II)-dependent step, thereafter converting into the stable WT species via a protein conformational change.[43]

In the present case, the reactivity of the initial capture complex appears to depend on the identity of the remaining cysteine residue. For C49A, the remaining C45 cys residue is likely positioned *trans* to the H135 residue since EXAFS analysis shows that C49A gives rise to a perfectly linear 2-coordinate species when reduced to the Cu(I) state. In this case, the preferred fate of the capture complex is to follow the pathway that leads to this stable reduced species, i.e. autoreduction. On the other hand in C45A, the remaining C49 ligand is likely in a *cis* configuration relative to the His residue such that reduction would lead to a less stable highly bent 2-coordinate structure which must pick up a third ligand to stabilize the Cu(I) form as is indeed observed by XAS of reduced C45A. In this case we propose that the favorable route is rearrangement to form the stable green Cu(II) species **3** with λ_{max} =365 nm. To achieve this, recruitment of additional protein-bound ligands would be required, and we suggest that His55 could fulfill this requirement. Such a rearrangement would also require conformational movements that could be slow. Thus some competition between rearrangement and autoredox reaction pathways would be expected, and could explain the presence of ∼30% Cu(I) in the final C45A Cu(II) product.

This reaction chemistry is supported by the EPR data which is consistent with the presence of two histidine ligands in the C45A green Cu(II) species, and by EXAFS data which also show evidence for imidazole outer-shell scattering in Cu(II)C45A. For C49A, the situation is more complex, since analogy to the H117/N42C variant suggests that the 380 nm absorption band could be assigned to more than one yellow species.[39] Indeed, the EPR data detect two distinct Cu(II) species with different electronic properties, and although EXAFS simulations appear to support a similar ligand set to C45A, the presence of multiple speciation makes it harder to draw firm conclusions. Therefore the identity of the yellow C49A Cu(II) species is somewhat obscure.

S K-edge absorption spectroscopy provides a measure of the covalency of the Cu−S bond through the intensity of the pre-edge transition which directly reflects the sulfur 3p character mixed into the $d_{x^2-y^2}$ orbital due to covalent bonding.[11,13] The renormalized pre-edge intensity of the WT protein is approximately 2.7 fold lower relative to that of the most intense plastocyanin, corresponding to ∼14% covalency per Cu−S bond in the Cu−S(Met) derivative. These results are correlated with the bond lengths in Table 3 which also contains comparisons to a number of other copper-cysteinate systems. The average covalency per Cu−S bond observed for the WT protein is comparable to the type 2 copper-thiolate tet-b, and lower than any cupredoxin. However, since the data only give the average covalency per Cu−S bond, it is possible that the actual covalency is different for Cu−S(C45) and Cu−S(C49). Although less reliable due to the unavoidable presence of Cu(I) from autoreduction chemistry, the measured covalency of the C45A variant (8% in the S(Met) derivative) is unexpectedly low, which may suggest that the Cu−S(C45) bond is significantly more covalent than that of Cu−S(C49). However, EPR simulations suggest the opposite result. Notwithstanding these complexities, the Cu−S covalency is more typical of type-2 Cu(II)-thiolates and supports the conclusion that WT Sco exhibits Cu−S interactions of low covalency, and argues against the presence of a covalent Cu−S pathway optimized for electron transfer. Therefore Sco proteins are unlikely to be involved in specific long-range electron transfer with a protein partner.

Resonance Raman provides an additional tool to interrogate the strength of the Cu−S bond. The WT protein resonance Raman spectrum is limited in its information content as the copper sulfur bond vibrations of the two cysteine residues are likely coupled. Notwithstanding, the average bond length calculated from Badgers rule agrees well with EXAFS simulations. The C45A variant spectrum is more informative, with a new intense feature at 352 cm^{-1}. This is most similar to the 355 cm^{-1} Cu−S resonance reported earlier for the H80C variant of superoxide dismutase (Table 4).[3] The Cu−S bond distance of ∼ 2.16 Å calculated from the intensity weighted average frequency is again close to the Cu−S distance of 2.15 Å derived from copper EXAFS simulation.

Table 4. Absorption and Resonance Raman Spectroscopic Features of WT BSco and Its C45A Variant Compared to Other Copper−Thiolate Proteins

Sample	λ_{max}, nm	RR frequencies (cm^{-1})	ref
Wt BSco (red)[a]	354, 450	320, **325**, 335, 378	This work
C45A-BSco (green)[a]	370, 460	320, 335, **352**, **378**	This work
Nitrosocyanin (red)[b]	390, 496	**310**, 340	5
H117G/N42C azurin (yellow)[a]	385	300, **323**, **341**, 359	39
H117G azurin[a]	420	267, **298**, **317**, 352, 362, 387, 404	55
SOD-Cu_2Cu_2H80C (green)[a]	459, 595	259, 279, 345, **355**, 396, 415	3
SOD-Cu_2Cu_2H80C (yellow)[a]	411, 604	283, 292, 335, **348**, 403	3
SOD-Cu_2Zn_2H120C[a]	406	283, 341, **359**, **366**, 401	3
SOD-Cu_2Zn_2H46C (pH 5.5)[a]	379	271, 298, 320, **342**, 378	3

RR spectra were obtained with [a] 413 nm excitation, and [b] 406.7 nm excitation. Frequencies in boldface denote the most intense peak(s) in the spectrum.

We were interested to determine whether the instability of the Cys variants could be rescued by mutation to histidine rather than alanine. This would create a ligand set similar to the cupredoxin (blue copper) family but in an unrelated protein scaffold. Our data show that both Cys to His variants are unstable and appear from EPR and EXAFS to exist in at least two molecular forms. Therefore the His_2Cys ligand set has no inherent stability on its own, but must be stabilized by an appropriate protein fold.

Conclusions

The $(Cys)_2His$ ligand set of BSco confers stability on the Cu(II) form of the wild-type protein. When either of the Cys residues is mutated to alanine, this stability is lost, leading to species which are susceptible to rearrangement or autoredox behavior. Similar conclusions were reported recently for the H135A variant.[27] Therefore, the Sco protein scaffold and/or the geometric arrangement of protein-derived ligands appears to confer special stability which is likely to be related to function. In our recent study of the reactivity and spectroscopy of the H135A variant we concluded that H135 was a critical element in the stability of the Cu(II) BSco site, and that mutation to Ala produced a species which was 3 orders of magnitude more sensitive to either autoredox or reduction by H_2O_2. We suggested that H135 might act as a redox switch, allowing a potent oxidative reactivity to be turned on by dissociation of the H135 ligand, which might in turn be initiated by interaction with a protein partner. It is clear from the present work that coordination of both Cys residues is also of crucial importance to the stability of the WT protein. Unlike the cupredoxins, the Sco Cu(II) site appears to be optimized to stabilize a bis-Cys configuration with only modest degrees of covalency. These features suggest a functional role very different from cupredoxins where the highly covalent Cu−S bond provides increased electronic coupling between donor and acceptor in electron transfer. The loss of function observed with C45A, C49A and H135A variants[20,22,23,27] appears to correlate more with destabilization of the native Cu(II) state than the Cu(I) state, suggesting that the Cu(II) form is critical to function. This finding limits functional alternatives to either redox reactivity, or to a metallochaperone function which involves *both Cu(II) and Cu(I) states*. The latter alternative offers an intriguing possibility that the mixed-valence Cu_A center can only be assembled via metalation using both oxidation states. Further studies are underway to explore these and other functional models.

Acknowledgment. We thank Dr. Martina Ralle for running mass spectra, and Dr. Pierre Moenne-Loccoz and Takahiro Hayashi for help with resonance Raman experiments. The work was supported by a grant to N.J.B. (GM54803) from the National Institutes of Health. This work was also supported at the Stanford Synchrotron Radiation Lightsource by the National Institutes of Health Biomedical Research and Technology Program Division of Research Resources, and by the U.S. Department of Energy Office of Biological and Environmental Research. The Illinois EPR Research Center (IERC) is supported by the University of Illinois, Urbana−Champaign.

Supporting Information Available: Eleven figures and one table, showing mass spectra of protein variants, oligomerization equilibria, autoreduction kinetics, EPR simulation of C49A, pH dependence of WT BSco, and EXAFS and EPR of Cys-to-His variants. This material is available free of charge via the Internet at http://pubs.acs.org.

JA910759V